THERMAL ANALYSIS OF THE ROTATIONAL MOLDING CYCLE FOLLOWED BY INTERNAL AIR TEMPERATURE PROFILES: AN APPLICATION FOR FOAMED POLYETHYLENE

F. J. Moscoso-Sánchez, J. Aguilar, R.M. Jiménez, J.R. Robledo-Ortíz, R. González-Núñez, Universidad de Guadalajara, Mexico
D. Rodrigue, Université Laval, Canada

Abstract

In this study, temperature profiles for the air inside the mold was measured to analyze the thermal behavior of a polymer for a complete rotational molding cycle. Foamed and unfoamed linear medium density polyethylene (LMDPE) parts were produced by biaxial rotational molding. A chemical blowing agent (azodicarbonamide, ACA) was used at different concentrations (0, 0.25, 0.50, and 1.0 % wt.). The temperature profiles inside the mold were measured for different oven temperatures (260-320 ^{o}C). The analysis proposed is based on the temperature profiles and their derivatives to better determine the different temperature transitions occurring in a complete molding cycle.

Keywords: Rotomolding, foam, temperature profile, molding cycle

Introduction

Rotational molding is a method to produce hollow plastic articles such as water tanks, kayaks, toys, etc. [1]. These parts are produced stress-free and without weld lines [2]. The vast majority of rotomolded parts today are optimized using internal air temperature (IAT) profiles as a first approximation to infer the state of the material inside the mold during processing [2-6]. Based on IAT profiles, physical transitions related to heat transfer can be determined [5,7].

The interest in rotational molding foaming has recently increased because lower weight, as well as better thermal and acoustic insulation can be obtained compared to unfoamed parts. Because the use of physical blowing agents (PBA) requires high pressures in the mold, they are not suitable for rotomolding. Therefore, chemical foaming agents (CBA) are generally preferred. The most used CBA is azodicarbonamide (ACA) due to its low toxicity, high gas yield (210 - 220 cm^3 of gas per gram of ACA) and the ability to match its decomposition temperature with the polymer´s processing temperature using suitable activators [8-10]. Moscoso *et al.* [11] studied the effect of blowing agent concentrations on linear medium density polyethylene (LMDPE) foams processed by rotational molding. Internal air temperature profiles were measured and showed that the blowing agent, due to its exothermic decomposition, slightly increased the peak IAT (PIAT) between 3 and 7°C for the range of conditions tested and the total cycle time increases from 79 to 98 min, while the density decreased from 0.931 g/cm^3 (0 phr ACA) to 0.295 g/cm^3 (1 phr ACA).

The main objective of this work is to analyze the internal air temperature (IAT) profiles for unfoamed and foamed polyethylene and to calculate their derivatives. Then, slope changes in the temperature profiles (first derivative) are used to evaluate more precisely the different transitions occurring in the polymer throughout the rotomolding cycle. Finally, the different processing stages (melting, crystallization and exothermic decomposition reaction of the chemical blowing agent) are compared with differential scanning calorimetry curves obtained under similar conditions.

Experimental

Materials

Linear medium density polyethylene (LMDPE) RO 93650 was supplied by Polimeros Nacionales (Mexico). This polymer has a melt flow index of 5.0 g/10 min (190 °C, 2.16 kg) and a density of 0.936 g/cm^3. Azodicarbonamide (ACA, $C_2H_4N_4O_2$) was used as the chemical blowing agent and supplied by Grupo-ALBE (Mexico). This grade of ACA is a yellowish fine powder (3 μm average particle size) with a density of 1.65 g/cm^3 and a decomposition temperature of 160 °C. Demolding agent CP-500 polyester resin was supplied by Poliformas Plasticas (Mexico).

Rotational Molding

Production of rotomolded parts was carried out in a laboratory-scale biaxial rotational molding machine with a cylindrical stainless steel mold of 3.6 mm wall thickness and a diameter of 19 cm with an overall length of 25.5 cm [12]. Dry-blends of LMDPE and ACA were prepared adding 0.0, 0.25, 0.5, and 1.0% wt. of ACA. Before loading the material, the demolding agent was applied to the internal surface of the mold. In all cases, a weight of 420 g of material (blowing agent and LMDPE) was loaded into the mold. The charged mold was then closed, mounted on the rotating arm, and introduced into the oven, which was pre-heated at different temperatures (260, 280, 300 and 320 ºC). Preliminary experiments varying rotating speeds and speed ratio were performed to

determine the best conditions leading to uniform wall thickness (Figure 1). According to the results of Figure 1, a rotational speed ratio of 1:4 was selected with a major axis speed of 3.5 rpm. The internal air temperature (IAT) was monitored with a thermocouple during the process. After the heating cycle, forced air cooling was started until the IAT dropped to 60 ºC for unfoamed samples and to 30 ºC for foamed ones. Finally, the part was demolded to start another cycle.

Morphological Characterization

Samples were cut from the rotomolded parts, frozen in liquid nitrogen, and fractured to expose their morphological structure. Scanning electron microscopy (SEM) was used to take images of the external surfaces, as well as cross-sections (exposed surfaces). The micrographs were taken at different magnifications using a Hitachi Tabletop TM-1000 SEM.

Differential Scanning Calorimetry

Differential scanning calorimetry (DSC) was carried out on a Perkin-Elmer DSC Pyres 6. Each sample went through a programmed heating profile between 20 and 250 ºC at rate of 5 ºC/min to be representative of the heat transfer rate inside the mold while processing. The transition temperatures were determined for LMDPE with and without ACA. The values of the melting, crystallization, and exothermic ACA decomposition temperatures with their respective enthalpies are reported in Table 1, as well as the amount of crystallinity (*% X*) which was determined as:

$$\% X = \frac{\Delta H_{EXP}}{\Delta H_{NEAT}} * 100 \qquad (1)$$

where ΔH_{EXP} is the experimental enthalpy and ΔH_{NEAT} is the enthalpy for neat 100% crystalline PE which is 293 J/g [13].

Results and discussion

Internal air temperature profiles as a function of processing cycle time at different oven temperature are presented in Figure 1 for rotomolded LMDPE. The oven temperature used were from between 260 and 320 °C with heating times between 15 and 25 min. At high oven temperatures (300 and 320 °C) the peak internal air temperatures (PIAT) obtained were between 203 and 215 °C. Under these processing conditions the molded parts were yellow-brownish due to polymer degradation [14]. Subsequently, the oven temperature was lowered to 260 and 280 °C for which the PIAT were between 125 and 180 °C. However, at 260 °C the polymer does not melt completely. Therefore, to ensure that the polymer was completely melted and did not degraded, it was decided to process this material at 280 °C and 20 min.

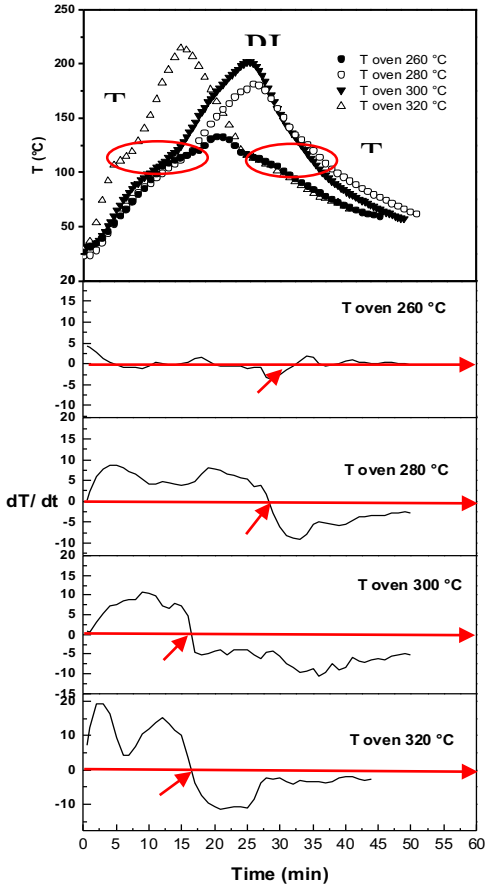

Figure 1. Internal air temperature (IAT) profiles and their derivatives as a function of time for LMDPE at different oven temperature and total cycle time. ■: 320 ºC, 49 min; •: 300 ºC, 53 min; ▲: 280 ºC, 55 min, and ◆: 260 ºC, 49 min.

Figure 1 shows the first derivative of the temperature profile as a function of time for different oven temperature (when complete parts were obtained). From these curves, the most important change detected, within experimental and calculation uncertainties, is the PIAT which is defined as the time for which the derivative is zero (changes from positive to negative values). The values are 180, 200 and 212 °C for oven temperatures of 280, 300 and 320 °C, respectively. But other important temperature transitions observed are: 1) the melting temperature (Tm) with values around 120 ºC for all oven temperatures, and 2) the crystallization temperature (Tc) with values around 110 ºC for all cases. As expected, these values are mostly constant since they depend on the polymer itself, which was kept constant here.

Micrographs were taken during different stages of the rotomolding cycle (Figure 2). The first micrograph (Fig.

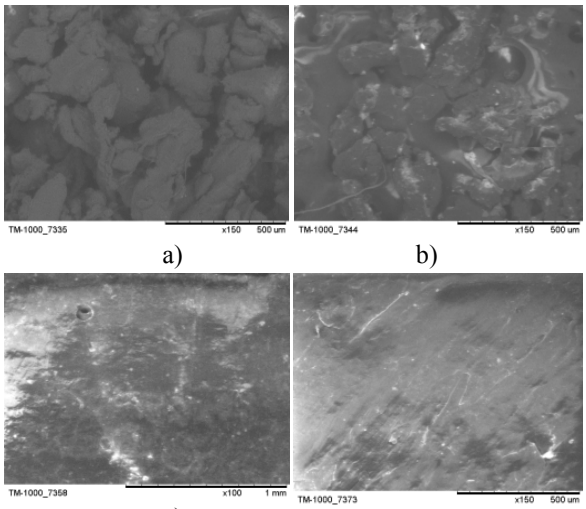

Figure 2. Micrographs of neat LMDPE taken at different stages of the rotomolding cycle for an oven temperature of 280 ºC: a) 5 min, b) 10 min, c) 15 min, and d) 20 min.

2A) was taking after only 5 min. At this stage the polymer inside the mold is not yet melted and still in a powder form. Subsequently, at 10 min, the thermal energy is absorbed by the material to begin the melting process (Figure 2b). In the micrograph of Figure 3c at 15 min, it can be seen that the polymer begins to consolidate. After 20 min, the temperature of the polymer inside the mold is above its meting point and the polymer mass is now consolidated.

In Figure 3, a qualitative analysis of the internal air temperature profiles was performed for foamed and unfoamed rotomolded parts. Due to high similarity of the curves in terms of temperature profiles, a calculation was performed to get their derivative and determine more carefully any changes in slope to find some relationships with the state of the material inside the mold as a function of temperature and time. This analysis is presented in Figure 3 for neat LMDPE and two ACA content (0.5 and 1%). The main stages of the rotomolded process are observed: induction of powder, adhesion to the mold walls around 10 min and with an IAT of 90 °C, melting-sintering of the powder pool between 10 and 15 min, fusion coupled with densification around 17 min and different temperatures (around 120 °C) depending on ACA content. From 10 to 17 min, the temperature increases from 93 to 120 °C where a substantial slope changes is observed. At this stage, the molten polymer is homogeneous and coalescence of solid particles starts under the action of surface tension [15] leading to a change of air temperature increase inside the mold (Figure 3).

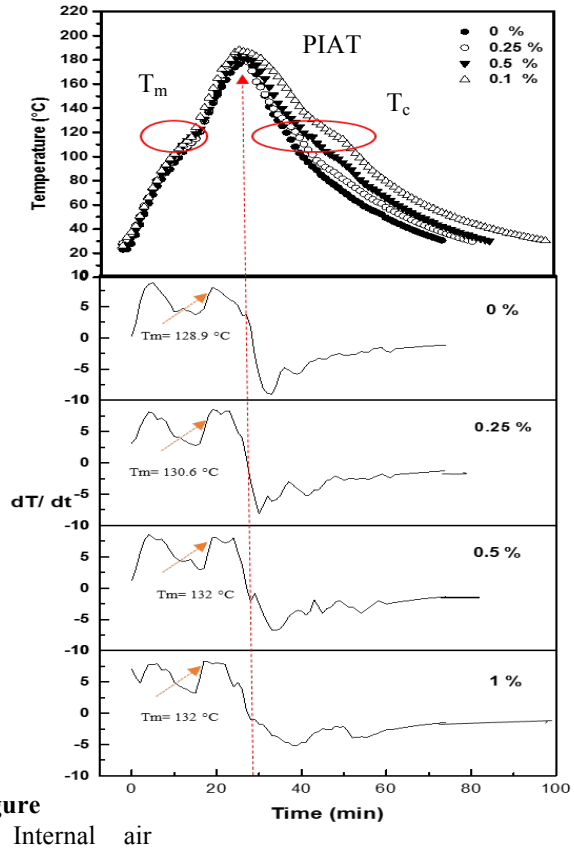

Figure 3. Internal air temperature (IAT) and derivatives as a function of time for unfoamed and foamed LMDPE at different ACA concentration.

In the last stage of the heating cycle (from 17 to 25 min), the temperature increases and the molten polymer facilitates the heat transfer and the air temperature increases to a maximum value (PIAT). The shift of the PIAT can be favored by the thermal decomposition of ACA, the observed values being: 181 ºC at 0% ACA, 185 ºC at 0.5% ACA, and 188 ºC at 1% ACA. According to Reyes-Labarta and Mancilla [16], the neat polymer matrix has an effect of thermal resistance in heat transfer, which contributes to a delay in the melting peak relative to the sample containing ACA. The ACA degradation reaction is heterogeneous and exothermic, and may introduce an effect of auto acceleration when the concentration of ACA in the sample increases. This can be associated to the production of cyanic acid generated from the decomposition reactions of ACA (auto-catalytic). This reaction can accelerate the ACA decomposition leading to changes in the temperature profiles as observed [16].

The morphology of the foamed and unfoamed rotomolded parts is presented in Figure 4. As expected, in

the case of neat LMDPE (Figure 4a) bubbles are not observed since the processing conditions were optimized.

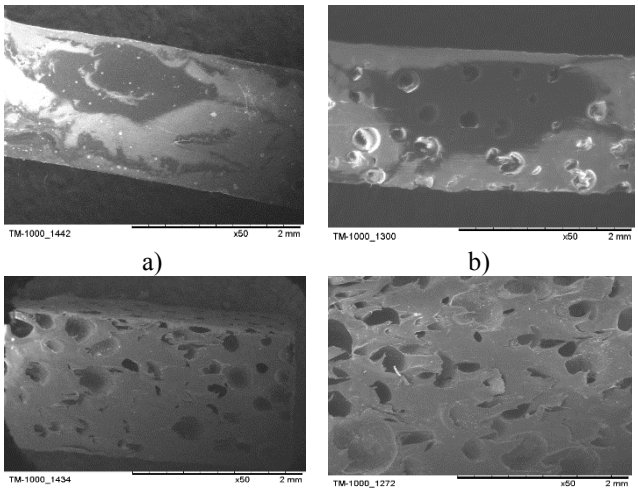

Figure 4. Micrographs of the final LMDPE morphology with different ACA content: a) 0%, b) 0.25%, c) 0.50%, d) 1.0% wt.

When ACA was added, the presence of bubbles in the micrographs is clear (Figure 4b, c, and d). As a result of successful foaming, an increase in part thickness is obtained as reported elsewhere [10].

The ACA decomposition kinetics were studied via DSC experiments [6,8,17]. Here, DSC tests were performed to identify each stage in the rotomolding process. Figure 5 presents a DSC trace of the sample with 1% ACA where three peaks can be observed. The first one (heating run around 129 ^{o}C) corresponds to the melting peak of LMDPE. The second one (heating run around 173 ^{o}C) represents the exothermic decomposition of ACA, while the third peak (around 113 ^{o}C) corresponds to LMDPE crystallization.

The heat fusion of LMDPE reported in Table 1 was evaluated to be around 144 J/g with a peak melting temperature of 129 °C, while the observed crystallization temperature was 113 °C with a crystallization enthalpy of around 160 J/g. These values do not change with ACA content for the range of conditions tested. For 0.5% ACA, the heat of heat reaction is around 2.5 J/g. However, at 1% ACA the heat of reaction increases substantially to about 7.5 J/g. Reyes-Labarta *et al.* [17], using DSC, studied the thermal decomposition of ACA in a mixture of PE and ACA and the minimum ACA content used was 0.99%. In this case, they reported a first reaction between 170 and 196 °C, followed by a second endothermic reaction at 255 °C. But this high temperature transition does not occur in our case since the PIAT were always below 220 ^{o}C.

From Table 1, the calculated crystallinity of neat LMDPE was below 60%, which is in agreement with the work of Liu and Tsai [18] for low linear density polyethylene (LLDPE) where values between 45 and 55% were

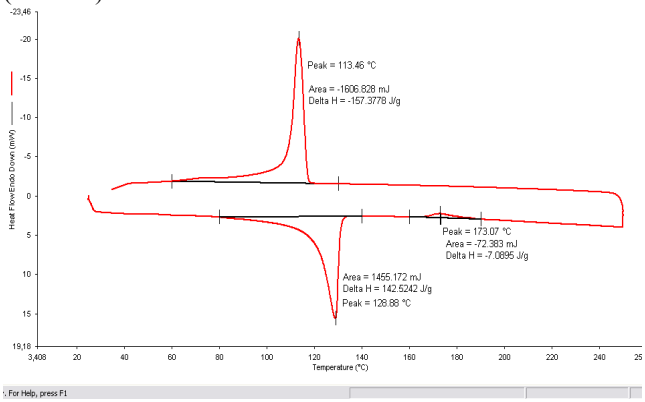

Figure 5. DSC of LMDPE with 1% ACA.

reported. For foamed LMDPE, the crystallinity level was about 55% and did not changed with ACA content as reported by Reyes-Labarta *et al.* [17].

Comparisons between the air temperatures at Tm and Tc from Figure 3 with the melting and crystallization temperatures obtained by DSC are reported in Table 1. In the case of neat LMDPE, the melting temperature obtained from derivative is the same at the obtained by DSC (128.9 °C). Also, the crystallization temperature at point Tc is located at 115 °C which is close with a value of 112 °C obtained by DSC. For LMDPE with ACA, the peak melting temperature obtained by DSC is around 129 °C compared to the values obtained by IAT at point Tm of around 130 °C (see Table 1). In the case of crystallization, the observed values by the IAT derivatives gives an average value of 112.5 ^{o}C compared to the values obtained by DSC (113 °C). So in general, there is a good agreement between the Tm and Tc values reported by the IAT derivatives and DSC measurements showing that the methodology is suitable to detect changes and a potential tool for the optimization of the rotomolding process.

Table 1. DSC analysis of LMDPE at different ACA contents.

ACA (%)	**0**	**0.25**	**0.5**	**1.0**
T_{melt} (ºC)	128.9	128.9	129.1	128.9
ΔH_{melt} (J/g)	147±1	144±1	146±1	138±5
T_{cryst} (ºC)	112	113	113	113
ΔH_{cryst} (J/g)	165±1	156±1	163±1	163±8
T_{foam} (ºC)	----	179	178	172
ΔH_{foam} (J/g)	----	2.5	2.4	7.05
X (%)	57±4	54±1	56±1	56±3
T_m (ºC)	128.9	129.5	130.6	132
T_c (ºC)	108	111	115	115

Conclusions

The thermal analysis of the internal profiles of air temperature and their derivatives offer a better understanding of the different stages of rotomolding when foam and unfoamed polyethylene parts were prepared. By means of the analogy between the internal profiles of air temperature and its derivatives, this analysis allow to determine slope changes with better accuracy at different stages. By performing differential scanning calorimetry (DSC), the information allowed to better describe the stages of melting, exothermic decomposition reaction of ACA, and crystallization in the thermogram. Good agreements between the melting and crystallization temperatures were observed by DSC measurements and IAT derivatives for foamed and unfoamed LMDPE parts. The amount of crystallinity for the prepared blends was not modified by the presence of ACA.

Acknowledgements

One of the authors (R. González-Núñez) acknowledges the financial support of the Mexican National Council for Science and Technology (CONACyT #259780) for a sabbatical year at the Université Laval.

References

1. Crawford R. J. and Throne J. L. Rotational molding technology, 1st ed. Norwich, NY: Elsevier Science & Technology, 2002.
2. Lim K. K., A. Ianakiev, J. B. Hull. *Rubber and Comp*, **32**, 421 (2003).
3. Revyako M. M., and E. Z. Khrol. *J Eng Phys & Thermophys*, **83**, 1089 (2010).
4. Nugent P.J., R. J. Crawford., and L. Xu. *Adv Polym Tech*, **11,** 181 (1992).
5. Cramez M. C., M. J. Oliveira., and R. J. Crawford, *Proc Instn Mech Engrs Part B: J Eng Manuf,* **217**, 323 (2002).
6. Liu S. J., and K. H. Fu. *J Appl Polym Sci,* **108**, 1696 (2008).
7. Ait Aissa A., C. Duchesne., and D. Rodrigue. *Polym Eng Sci.* **52**, 953 (2012).
8. Marcilla A., J. C. García-Quesada, M. I. Beltran, R. Ruiz-Femenia. *J Appl Polym Sci*. **107**, 2028 (2008).
9. Klempner D. A. F., and C. Kurt. Handbook of Polymeric Foams and Foam Technology; Hanser: Munich (1991).
10. Moscoso-Sánchez F. J., E. Mendizabal, C. F. Jasso-Gastinel, P. Ortega-Gudiño., J. R. Robledo-Ortíz., R. González-Núñez and D. Rodrigue. *J Cell Plast*, **32**, 199 (2014).
11. Robledo-Ortiz J. R., C. Zepeda, C., Gómez., D. Rodrigue., R. González-Núñez. *Polym Testing* **27**, 730 (2008).
12. López-Bañuelos R. H., F. J. Moscoso., P. Ortega-Gudiño., E. Mendizabal., D. Rodrigue., R. González-Núñez. *Polym Eng Sci*, **50**, 7 (2013).
13. Mark H. F. *Ed* Encyclopedia of Polymer Science and Engineering, Wiley NY (1990).
14. Petchwattana N., S. Covavisaruch., and S. Chanakul. *J Polym Res,* **19**, 9921 (2012).
15. Bellehumeur C., Kontopoulou M., and Vlachopoulos J. Rheol. Acta, **37**, 270 (1998).
16. Reyes-Labarta J. A., and A. Marcilla. *J Appl Polym Sci,* **107**, 339 (2008).
17. Reyes-Labarta, J. A., M. M. Olaya and A. Marcilla. *J Appl Polym Sci* **102**, 2015 (2006).
18. Liu S. J., and Tsai CH. *Polym Eng Sci* **39**, 1776 (1999).